NMR Studies on Intercalation Compounds of Layered Chalcogenides with Methylamines and Ammonia

M. Molitor*, W. Müller-Warmuth, H. W. Spieß**
Institut für Physikalische Chemie der Universität Münster
R. Schöllhorn
Anorganisch-Chemisches Institut der Universität Münster

Z. Naturforsch. **38 a**, 237–246 (1983); received December 6, 1982

Dedicated to Professor Alfred Klemm on the occasion of his 70th birthday

NMR wideline and pulse techniques have been used to study orientation and molecular motions of the intercalation compounds of niobium disulfide with monolayers of mono-, di-, and trimethylamine, tetramethylammonium and ammonia. Specific information has been obtained from the ^1H and ^2D spectra and from spin-lattice relaxation measurements of the selectively deuterated monomethylamines. Models for the arrangement of the various molecules within the layers and for the motions have been derived. One-dimensional rotation of CH_3 and NH_3 groups, rapid intermolecular exchange of NH, NH_2 and NH_3 protons, as well as translational and reorientational motions of whole molecules are of importance. Interpretation of spin-lattice relaxation rates at various temperatures and frequencies yields details of some of these motion and numerical values for the activation energies.

1. Introduction

From both the chemical point of view and the aspect of technical application there has been considerable interest in intercalation compounds which are formed by the insertion of atomic of molecular guest species into suitable host lattices [1]. The chemical process associated with intercalation into conducting host lattices may be considered as a reversible topotactic redox reaction by electron/ion transfer, and stoichiometric or nonstoichiometric crystalline compounds can thus be obtained. Among various host lattices with different structure and dimensionality layered transition metal (M) dichalcogenides MX_2 in particular are capable of intercalating a large variety of molecular species of different size and geometry. The host lattice has hexagonal structure and can be described in terms of a stacking of MX_2 sheets which are held together by weak van der Waals forces. The conduction electrons in the layers display quasi-two-dimensional properties. Upon intercalation the lattice is expanded perpendicular to the layer planes depending on the size and orientation of the guest species. The properties of the guest phase are strongly influenced by the nature of the guest-host and guest-guest interactions and the two-dimensional character of the interlayer space.

For studying structure and motion of such intercalation compounds nuclear magnetic resonance (NMR) techniques have proved to provide powerful tools. We investigated in particular the structure of the guest phase and the mobility of water in various layered chalcogenides of the type $A_x^+(H_2O)_y[MS_2]^{x-}$ with A = Li, Na, K, NH_4, Rb, Cs [2, 3]. In the monolayer hydrates the diffusion turned out to be two-dimensional in character and proton exchange within the layers was shown to exist [4]. We have now extended such investigations to molecular intercalates with Lewis base character, and we present here results of a study of the intercalation compounds of niobium disulfide NbS_2 with monolayers of mono-, di-, and trimethylamines, tetramethylammonium ion and ammonia itself. The aim was to gain information on the molecular dynamics and orientation of the guest species and on the guest-host and guest-guest interactions, respectively, by solid state NMR techniques. In principle the spectra and the spin-lattice relaxation were expected to depend on interactions associated with

* Present address: Schott Glaswerke, Mainz.
** Present address: Institut für Physikalische Chemie der Universität Mainz.

Reprint requests to Prof. Dr. W. Müller-Warmuth, Institut für Physikalische Chemie der Universität Münster, Schlossplatz 4/7, D-4400 Münster.

0340-4811 / 83 / 0200-0237 $ 01.3 0/0. – Please order a reprint rather than making your own copy.

i) one-dimensional rotation of CH_3 or NH_3 groups about their threefold (C_3) symmetry axes,
ii) reorientation of the molecular symmetry axes within the layer,
iii) two-dimensional diffusion of molecules, and
iv) proton-exchange.

The question whether rapid proton exchange occurs is closely connected with the postulated existence of ionic species [5], vide infra. The results for $NH_3[NbS_2]$ will be compared with those for $NH_3[TaS_2]$ obtained from extensive studies of Silbernagel et al. [6–11].

2. Preparation of Samples

Host lattice

Niobium disulfide was obtained by reaction of the elements (purity: sulfur 99.5%, niobium 99.9%) in evacuated sealed quartz ampoules at 950 °C/8 d under addition of iodine (5 mg/ml ampoule volume) for isothermal transport. The ratio Nb/S was equivalent to 1:2.1. After the reaction iodine and excess sulfur were removed by treatment of the resulting product in vacuum at 150 °C/10^{-2} bar. The size range of the crystallites corresponded to 0.05–0.1 mm. Hexagonal lattice parameters of the product 2H-NbS_2 were a = 332.1 pm, c = 1188 pm.

Ammonia and monomethylamine compounds

These phases were prepared by thermal intercalation of NbS_2 with the corresponding guest species in a vacuum system. For removal of traces of H_2O and O_2 ammonia was first condensed on sodium metal and subsequently allowed to react with 2–3 g of outgassed NbS_2 close to the temperature of the boiling point of NH_3 in a vycor glass ampoule of appropriate size. After a reaction time of 8 h the temperature was slowly increased to 25 °C and the ampoule was sealed.

The gaseous monomethylamines CH_3NH_2, CH_3ND_2 and CD_3NH_2 were prepared from the commercially available hydrochlorides by reaction with aqueous solutions of NaOH or NaOD, respectively, and condensed on freshly prepared CaO. To remove the last traces of water, the amines were subsequently condensed on sodium metal and stirred until the intense blue color of the metal/amine solution appeared. The following procedure was similar to that described above for the ammonia phase.

Compounds with higher methylamines

The preparation of these phases was achieved by electrochemical intercalation at ambient temperature. Pressed polycrystalline electrodes of NbS_2 (2–3 g) were reduced cathodically under N_2 atmosphere in aqueous 1 M solutions of dimethyl-, trimethyl- and tetramethylammonium sulfate at constant current. X-ray data and potential/charge transfer curves indicated for all systems a two phase region up to $n \sim 0.3$ e^-/NbS_2, followed by a non-stoichiometric region at higher values of n. The resulting products were washed with N_2 saturated water to remove the electrolyte, dried at 10^{-2} mbar/25 °C and sealed in glass ampoules under inert gas.

Characterization

The composition of the intercalated phases was checked by microanalysis (C, H, N) and gravimetric determination of the Nb content (Nb_2O_5). From the hexagonal lattice parameters (X-ray Guinier photographs) the interlayer spacing values were obtained. The data are summarized in Table 1.

Table 1. Characterization of amine intercalation compounds G_x $[NbS_2]$. G = guest species, x = nominal ratio guest molecule/NbS_2 as determined from the C/N content, d = interlayer spacing, n = electrochemical charge transfer in e^-/NbS_2.

G	x	d(pm)	n
NH_3	1.0	902	–
CH_3NH_2	0.5	934	–
CH_3ND_2	0.5	934	–
CD_3NH_2	0.5	935	–
$(CH_3)_2NH_2^+$	0.33	969	0.34
$(CH_3)_3NH^+$	0.3	962	0.30
$(CH_3)_4N^+$	0.28	1141	0.31

3. Experimental Results

The ^1H wideline measurements were carried out with a homemade spectrometer operated at 8 MHz. The signals were measured as derivated curves of the absorption lines, then averaged and stored in a computer of average transients. ^2D NMR signals were measured at 13.5 MHz using a Bruker SWL 3–100 wideline spectrometer equipped with a Datalab DL 400 signal averager. For the T_1 measurements a Bruker variable frequency pulsed NMR

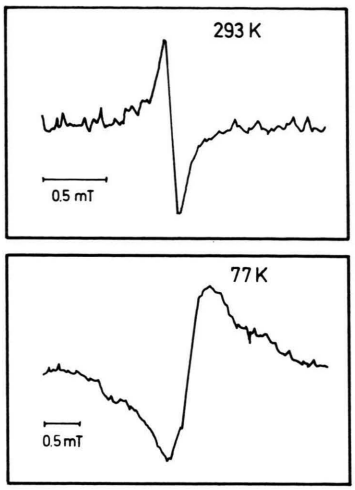

Fig. 1. ^{1}H-NMR spectrum (derivative curve) of $(CH_3NH_2)_{0.5}[NbS_2]$ measured at two different temperatures.

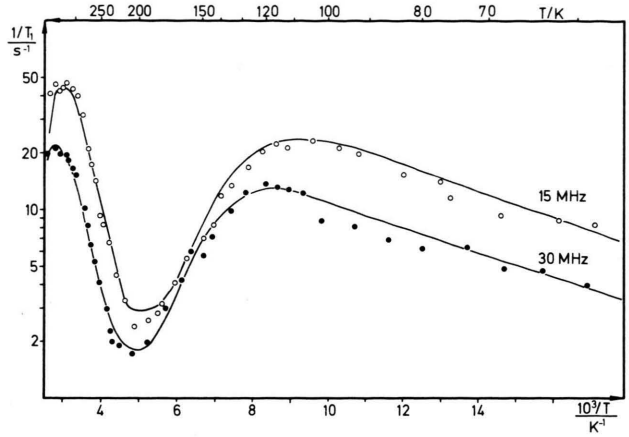

Fig. 2. Proton spin-lattice relaxation rate versus reciprocal temperature for $(CH_3NH_2)_{0.5}[NbS_2]$.

spectrometer and 90°-τ-90° pulse sequences were employed. The samples were placed in different variable temperature nitrogen or helium flow cryostats depending on the temperature range in question.

$(CH_3NH_2)_{0.5}[NbS_2]$

At room temperature the ^{1}H NMR spectrum for a powder sample of methylamine intercalated in niobium disulfide layers consists of an intense central line with poorly resolved shoulders (Figure 1). Upon cooling the signal broadens from $\delta H =$ 0.11 mT to 0.58 mT, where δH denotes the magnetic field separation between derivative maxima of the absorption spectrum (Fig. 1, below). The second moment of the absorption line increases from 0.014 $(mT)^2$ to 0.24 $(mT)^2$. Figure 2 shows the temperature dependence of the spin-lattice relaxation rate $1/T_1$ measured at two different NMR frequencies and plotted against reciprocal temperature. The $\log(1/T_1)$ vs. $(10^3/T)$ curves appear to be greatly asymmetric and extend to lower temperature. The solid lines correspond to the data fits discussed in the next chapter.

$(CD_3NH_2)_{0.5}[NbS_2]$ and $(CH_3ND_2)_{0.5}[NbS_2]$

In order to understand the observed behaviour we prepared and studied analogous materials with selectively deuterated methylamines. The proton resonance of CH_3ND_2 looks rather similar to that of Fig. 1, but the satellite lines having a separation of $\Delta H = 0.37$ mT are now well resolved (Figure 3a). The ^{1}H NMR spectrum of CD_3NH_2 consists of a narrow line only (Figure 3b). At low temperature the ^{1}H NMR spectra of both CH_3ND_2 and CD_3NH_2 broaden considerably (not shown).

The ^{2}D spectrum of CD_3NH_2 shows the powder line shape characteristic of an $I = 1$ spin system subject to an axially symmetric quadrupole coupling [12]. The most prominent features are the singularities leading to a doublet in the derivative mode

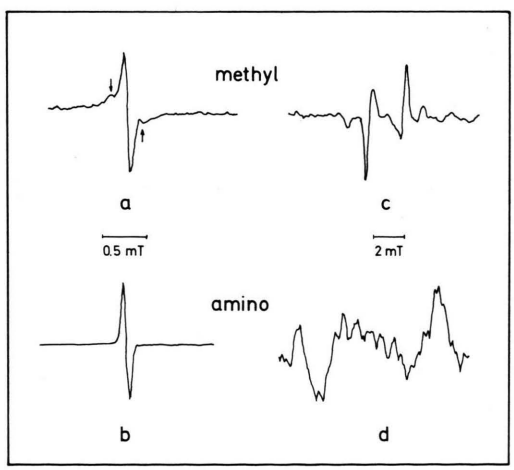

Fig. 3. ^{1}H-NMR (left hand side) and ^{2}D-NMR spectra (right hand side) of the methyl and amino group, respectively, of $(CH_3NH_2)_{0.5}[NbS_2]$. Selectively deuterated compounds were used.

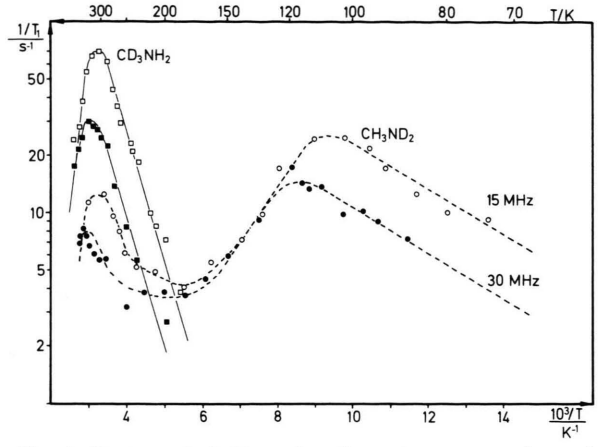

Fig. 4. Proton spin-lattice relaxation rate versus reciprocal temperature for $(CD_3NH_2)_{0.5}[NbS_2]$ (solid line) and $(CH_3ND_2)_{0.5}[NbS_2]$ (dotted line). The measurements were carried out at 15 MHz (○, □) and 30 MHz (●, ■).

with a splitting of $\Delta H = 2.9$ mT, accompanied by satellites exhibiting twice this splitting, Figure 3c. The deuteron spectrum of the amino group in CH_3ND_2 shows a similar pattern, the central part of which with a splitting of approximately 8 mT is displayed in Figure 3d. Note the difference to the proton spectrum, where a narrow central line only is observed, Figure 3b.

As compared with CH_3NH_2, in the temperature dependence of $1/T_1$ for CD_3NH_2 only the high temperature maximum is left (Figure 4). For CH_3ND_2 the low temperature maximum is more or less identical with that of CH_3NH_2, whilst the high temperature peak is much weaker.

$((CH_3)_2NH)_{0.3}[NbS_2]$, $((CH_3)_3N)_{0.3}[NbS_2]$ and $[(CH_3)_4N^+]_{0.3}[NbS_2^-]$

Figure 5 shows the ^{1}H NMR spectra measured at room temperature. The spectrum of dimethylamine is of the same type as that of methylamine, but the separation between the satellites is smaller (0.21 mT). Trimethylamine has a rather broad and structureless line and tetramethylammonium a very narrow signal. At 77 K the spectra appear to be much broadened (not shown) and the second moments become 0.11 $(mT)^2$, 0.08 $(mT)^2$ and 0.20 $(mT)^2$, respectively. The corresponding values at room temperature are 0.002 $(mT)^2$ and 0.024 $(mT)^2$; for $(CH_3)_4N^+$ it is smaller.

The temperature dependences of $1/T_1$ (Figs. 6 to 8) are distinguished by a similar character as that of

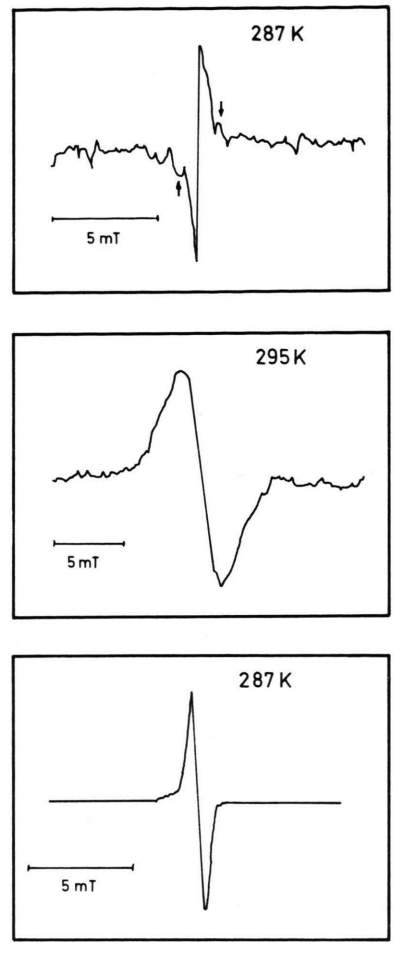

Fig. 5. ^{1}H-NMR spectra of a) $((CH_3)_2NH)_{0.3}[NbS_2]$, b) $((CH_3)_3N)_{0.3}[NbS_2]$, and c) $((CH_3)_4N^+)_{0.3}[NbS_2]$.

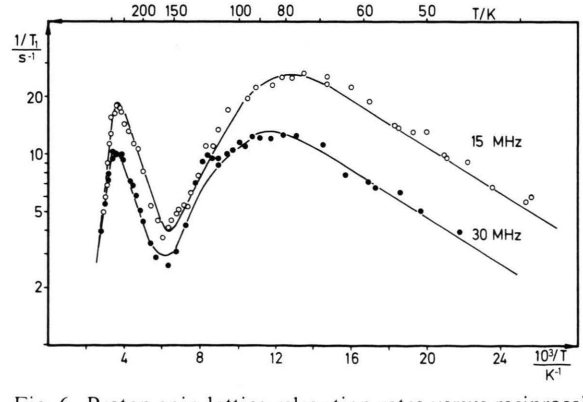

Fig. 6. Proton spin-lattice relaxation rates versus reciprocal temperature for $((CH_3)_2NH)_{0.3}[NbS_2]$.

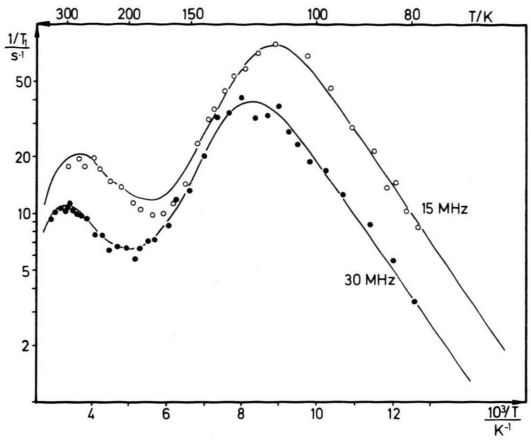

Fig. 7. Proton spin-lattice relaxation rates versus reciprocal temperature for $((CH_3)_3N)_{0.3}[NbS_2]$.

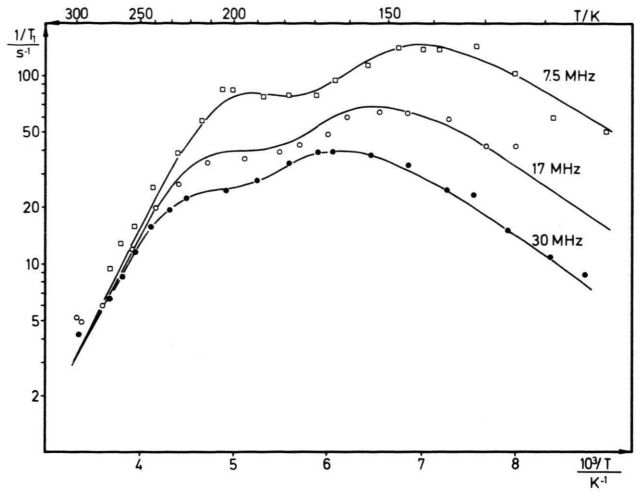

Fig. 8. Proton spin-lattice relaxation rates versus reciprocal temperature for $((CH_3)_4N^+)_{0.3}[NbS_2]$.

methylamine, but the maxima occur at different temperatures, and in case of $(CH_3)_4N^+$ there is more overlap between the two curves.

$NH_3[NbS_2]$, $(NH_3)_{0.5}[NbS_2]$ and $NH_3[TaS_2]$

We have also studied several intercalation compounds with ammonia itself since the results for the methylamines could be expected to be useful for the understanding of some problems still open after the comprehensive work of Silbernagel et al. [6–11]. The wideline spectra of $NH_3[NbS_2]$ correspond to those observed in TaS_2 and TiS_2 [8, 9], but the temperature dependence of the relaxation rate $1/T_1$ (Fig. 9) is much more similar to that of $((CH_3)_4N^+)_{0.3}[NbS_2^-]$ rather than to that published for $NH_3[TaS_2]$ [10, 11]. We therefore repeated the measurements for $NH_3[TaS_2]$, obtaining essentially the same results as those of Ref. [10] with one maximum only. Finally measurements were made on a sample $(NH_3)_{0.5}[NbS_2]$ which was not fully intercalated. In contrast to measurements published for $(NH_3)_{0.8}[TaS_2]$ [11], giving results not much different from those of the fully loaded material, Fig. 10 shows that the maxima are shifted towards lower temperature and that the relaxation strengths are different.

3. Interpretation

3.1. Wideline Spectra

Analysis of the spectra is facilitated by considering first the selectively deuterated methylamines of Figure 3. The ^1H NMR powder spectrum of the *methyl group* (Fig. 3a) corresponds to the dipolar lineshape calculated for a triangular configuration of protons when isolated CH_3 groups rotate about their threefold (C_3) axes with a frequency larger than the frequency splitting in the experiment [13]. For such a situation the spectrum consists of a central line and two satellites with a magnetic field splitting of

$$\Delta H = \frac{3}{2}\left(\frac{\mu_0}{4\pi}\right)\cdot\frac{\gamma_p\,\hbar}{R^3}\,. \qquad (1)$$

Using the values $\mu_0/4\pi = 10^{-7}$ SI units, $\gamma_p = 2.675 \cdot 10^8\,T^{-1}\,s^{-1}$ (magnetogyric ratio of the proton),

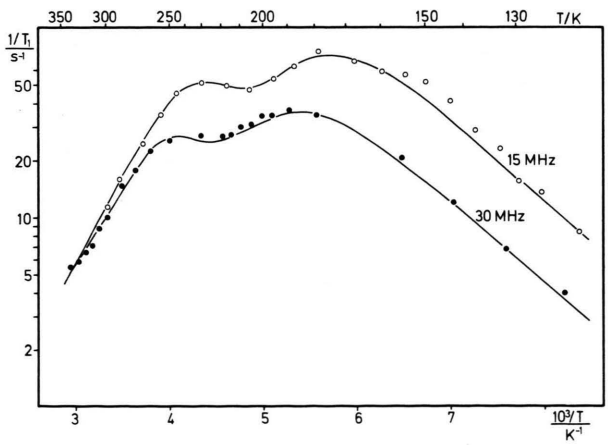

Fig. 9. Proton spin-lattice relaxation rates versus reciprocal temperature for $NH_3[NbS_2]$.

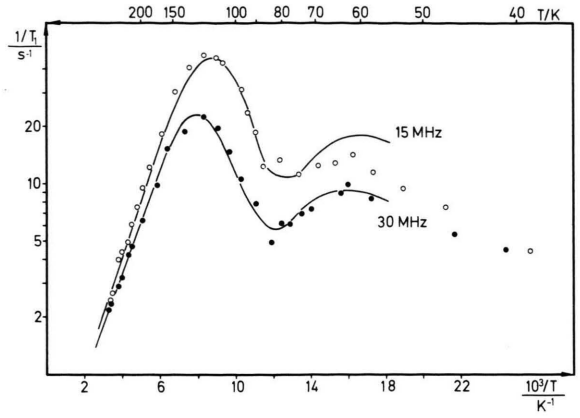

Fig. 10. Proton spin-lattice relaxation rates versus reciprocal temperature for $(NH_3)_{0.5}[NbS_2]$.

$\hbar = 1.0545 \cdot 10^{-34}$ Js (Planck's constant) and $R = 0.179$ nm (proton-proton distance) Eq. (1) yields a splitting of 0.74 mT, which is twice as much as that observed experimentally. This means that there is an additional reduction by a sufficiently rapid reorientation of the whole molecules about another axis. In such a case the right hand side of Eq. (1) has to be multiplied by a factor $\frac{1}{2}(3\cos^2\Theta - 1)$, where Θ is the angle between the axis about which the molecule rotates and the C_3 direction. The experimental results are consistent with $\Theta = 90°$, i.e. reorientation takes place about the crystallographic c axis, see Fig. 11 (next chapter).

This interpretation is supported by the ^{2}D NMR spectrum of the CD_3 group, Figure 3c. In this case the theory of the ^{2}D NMR is similar to that of the ^{1}H NMR of a proton-proton pair [14], and a doublet is found with a magnetic field splitting of [15]

$$\Delta H = \frac{3}{4}\frac{e^2 q\, Q}{\gamma_D \hbar}. \qquad (2)$$

eQ is the quadrupole moment, and eq is the electric field gradient at the ^{2}D nuclei, which is first of all determined by the electrons within the C–D bonds and which is assumed to be axially symmetric. Experimental values of the quadrupole coupling constant e^2qQ/h published for rotating CD_3 groups in solids normally lie between 50 and 60 kHz [15, 16]. This corresponds to splittings between 5.9 and 6.9 mT ($\gamma_D = 4.106 \cdot 10^7\ T^{-1}\ s^{-1}$), cf. (2). Of course, the reorientational motion about the c axis again reduces these values by a factor 2, so that there is satisfactory agreement with our experimental value of 2.9 mT.

The proton resonance of the *amino group* is a single narrow line (Fig. 3b) rather than a two-spin doublet which was observed for water in layered chalcogenides [2]. The singulet can neither be explained in terms of a NH_2 rotation, nor by any kind of isotropic random motion, since the ^{2}D spectrum of the amino group (Fig. 3d) is a doublet. For rigid ND_2 groups experimental values for quadrupole coupling constants e^2qQ/h between 125 and 195 kHz have been published [15, 16], depending upon whether hydrogen bonds exist or not. The electric field gradient is approximately axially symmetric, since it is dominated by the electrons within the N–D bonds. In our case, therefore a splitting between 14 and 22 mT would be expected, cf. (2), when the molecular rotation about the c axis is not yet considered. The latter reduces the values by $\frac{1}{2}(3\cos^2\Theta - 1)$ with $\Theta = 35.3°$, see Fig. 11. Thus a field splitting between 7 and 11 mT is expected in satisfactory agreement with our experimental value of 8 mT.

It remains to explain the narrow ^{1}H NMR line, and here intermolecular proton exchange is the only mechanism which is not at variance with the experiments. Indeed, proton exchange has been shown to exist even in the analogous monolayers of water [4].

The ^{1}H NMR of CH_3NH_2 intercalated in NbS_2 layers (Fig. 1) is just the superposition of the spectra of Figs. 3a and 3b. Since the central resonance contains large contributions from both the methyl and the amino protons the satellites cannot easily be recognized. At low temperature broadening occurs since several modes of molecular or protonic motion are frozen out.

The aforementioned results also explain the narrow lines observed for $NH_3[NbS_2]$ and for $NH_3[TaS_2]$, where the latter was interpreted by a molecular motion which averages the proton-proton dipolar interactions to zero [8]. As in the case of intercalated methylamine, however, the narrow and symmetric powder spectrum of ammonia at room temperature can readily be understood in terms of a rapid proton exchange. This interpretation agrees well with data of Silbernagel et al., not only as far as the ^{2}D spectrum is concerned [9], but also with respect to the anisotropy of the spin-lattice relaxation time [7].

The ^{1}H NMR spectrum of $((CH_3)_2NH)_{0.3}[NbS_2]$, Fig. 5a, looks rather similar to that of the intercalation complex of methylamine. The spectrum again is determined by both the rotating three-spin system of the methyl protons and the exchange-narrowed line from the amino proton, where the splitting is further reduced by molecular reorientation about the c axis. The smaller magnetic field splitting of 0.21 mT indicates that the angle Θ between the C_3 axis and the c axis is about 113° which is in complete agreement with the arrangement of Fig. 11, where the lone pair orbital of the nitrogen atom lies parallel to the disulfide layers. The two outer lines that can be recognized in Fig. 5a are probably due to intercalated water impurities.

No specific information is obtained from the structureless signal of $(CH_3)_3N[NbS_2]$, Fig. 5b, probably because of the various intra- and intermolecular interactions between the methyl protons. The ^{1}H NMR line of $(CH_3)_4^+N[NbS_2^-]$, Fig. 5c, is again narrow, and this mirrors the high symmetry of the intercalated molecules which makes the reorientational motion more ore less isotropic. The second moment values of the intercalation complexes at 77 K show that (in contrast to molecular reorientation, exchange, and diffusion) the rotations of the methyl groups are not yet completely frozen out.

3.2. Spin-Lattice Relaxation Data

With the exception of intercalated CD_3NH_2 (Fig. 4) all the log $1/T_1$ vs. $10^3/T$ representations (Figs. 2, 6–10) display two maxima of the relaxation rates. Assignment is achieved by comparing the data of monomethylamine (Fig. 2) and its selectively deuterated derivatives (Figure 4). The "low" temperature peak which occurs in Fig. 2 between 110 and 120 K disappears upon deuteration of the methyl group, Figure 4. From this and also from general considerations it is clear that in Figs. 2 and 6 to 8 the "low" temperature peak belongs to the hindered rotation of the methyl groups about the C_3 symmetry axes, and the "high" temperature peak is associated with the reorientation and translation of the molecules. Those protons which do not participate in the respective motion in the temperature range in question will be relaxed via spin diffusion [12] to the center of thermal motion. The assignment of the relaxation peaks for ammonia (Figs. 9 and 10) is more involved. By analogy with the methylamines the "high" temperature peak is assumed to be associated with the reorientation and translation of the NH_3 molecules, and the "low" temperature relaxation could be associated with the rotation of NH_3 about the symmetry axis.

The data can neither be explained in terms of the simple BPP relation [17]

$$1/T_1 = C\left[\frac{\tau_c}{1+\omega^2\tau_c^2} + \frac{4\tau_c}{1+4\omega^2\tau_c^2}\right], \tag{3}$$

nor by the ln-dependence, derived for a two-dimensional diffusion [18]

$$1/T = C\left[\tau_c \ln\left(1+\frac{1}{\omega^2\tau_c^2}\right) + 4\tau_c \ln\left(1+\frac{1}{4\omega^2\tau_c^2}\right)\right], \tag{4}$$

which has been verified experimentally in the analogous monolayer hydrates [4]. In the present work two-dimensional diffusion was only observed in the sample $(NH_3)_{0.5}[NbS_2]$, which is not fully intercalated, cf. Figure 10. Here the solid line corresponds to Eq. (4) with a relaxation strength $C = 1.9 \cdot 10^9\ s^{-2}$ and an activation energy $E_A = 7.5$ kJ/mol. As usual the correlation time τ_c of the respective motion is connected with the temperature by an Arrhenius law

$$\tau_c = \tau_{c0}\, e^{E_A/RT}. \tag{5}$$

In the fit of Fig. 10 a prefactor $\tau_{c0} = 1.2 \cdot 10^{-12}$ s was used.

All the other relaxation peaks are distinguished by different apparent activation energies at temperatures above and below the $1/T_1$ maximum. Moreover, below the maxima the $1/T_1$ values are not proportional to the square of the Larmor frequency ω as required by Eqs. (3) and (4). A similar experimental behaviour was found for molecular or ionic motion in glasses [19, 20], biological materials [21] and several other samples which are listed e.g. in [22]. It is possible to explain all this data in terms of an asymmetric distribution of correlation times [19–21] or by a phenomenological modification of the BPP theory [22, 23]. In the second case it has been suggested that one may write, at temperatures below the maximum, a simple power law,

$$1/T_1 \sim \tau_c/(\omega\tau_c)^{\alpha+1}.$$

We have applied this treatment and generalized the phenomenological formula in order to obtain BPP

behavior at temperatures above the maximum as observed experimentally

$$1/T_1 = C\left[\frac{\tau_c}{1+(\omega\tau_c)^{\alpha+1}} + \frac{4\tau_c}{1+(2\omega\tau_c)^{\alpha+1}}\right]. \quad (6)$$

For $\alpha = 1$ Eq. (6) reduces to the BPP formula. At temperatures below the maximum the apparent activation energy is αE_A, and the ratio of relaxation times at two different Larmor frequencies is $T_1(\omega_1)/T_1(\omega_2) = (\omega_1/\omega_2)^{1+\alpha}$.

Our experimental data of Figs. 2 and 6 to 10 can be fitted by the expressions given in Eqs. (5) and (6). There is, within experimental error, complete agreement as far as temperature and frequency dependence are concerned. The parameters thus obtained for both relaxation peaks of each sample are listed in Table 2, and the fits are shown in the figures by solid lines.

4. Discussion

4.1. Orientation of Guest Molecules within the Layers

The precise orientation of the methylamines can be derived from the NMR spectra, as described above, and the lattice expansions. Figure 11 gives a schematic representation for each of the intercalated molecules. These are drawn on scale as far as the size of the amine molecule and the expansion of the van der Waals gap (Table 1) are concerned. Only one of the respective molecules, which are arranged two-dimensionally in the gap, is shown. For CH_3NH_2 and $(CH_3)_2NH$ the axis of the lone pair orbital of the nitrogen atoms always lies parallel to the disulfide layers and, as already stated, hindered internal rotations of the methyl groups and reorientational motion of the molecules about the axes indicated in the figure take place. In addition there is translational diffusion. The position with the lone pair orbital parallel to the layers is energetically favourable, but it was only found for the smaller molecules intercalated in NbS_2. In case of $(CH_3)_3N$, for steric reasons, as revealed by the gap expansion observed, the axis of the lone pair orbital of the nitrogen atom has to be perpendicular to the layers; otherwise the expansion should be 545 pm rather than the experimental value of 362 pm. $(CH_3)_4N^+$ finally has cubic symmetry and the motion is believed to be more or less isotropic.

NH_3 is also included in Figure 11. All the experiments, including those of Silbernagel et al. [6–11],

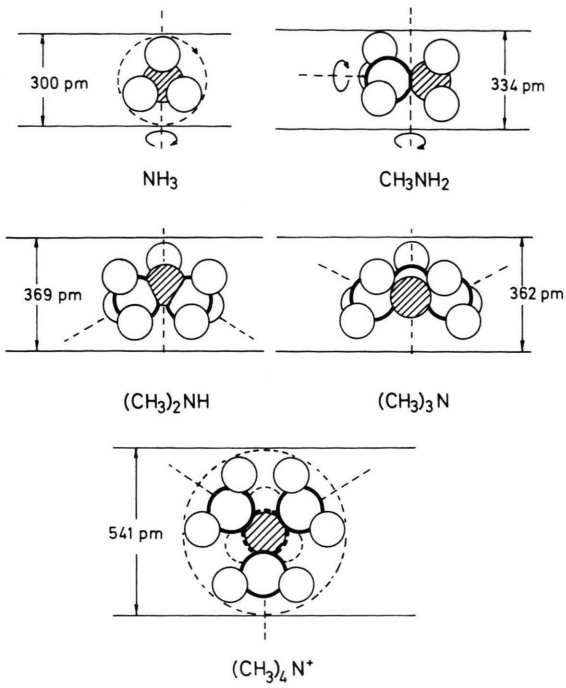

Fig. 11. Schematic representation of the arrangement and motions of the various molecules between the disulfide layers.

for $NH_3[TaS_2]$ and the analogy with CH_3NH_2 fully agree with the proposed position, where one-dimensional rotation of the NH_3 group, reorientational motions of the molecule, diffusion and proton exchange make this molecule a complicated object to study.

4.2. Intermolecular Proton Exchange

The existence of intermolecular proton exchange has been directly shown to exist for CH_3NH_2. In a monolayer arrangement rapid proton exchange is not at all obvious, but it was already observed in monolayers of water [4]. For chemical reasons the existence of rapid proton exchange requires the presence of ionic species, and we believe that a certain fraction of the amines occur protonated as cations, where the electrons are transferred to the NbS_2 layers. This is in agreement with an earlier investigation of the mechanism of NH_3 intercalation into TaS_2 [5] which demonstrated that the corresponding redox process involves the oxidation of a fraction of the guest molecules with formation of N_2, H^+ and finally NH_4^+. About 10% NH_4^+ cations

Table 2. Numerical results for the relaxation strength C, the activation energy E_A, the distribution parameter α, and the limiting value of the correlation time τ_{CO} as obtained from the best fitting curves after Eq. (6) for the relaxation maxima at "high" and "low" temperatures.

Fig. No.	Guest molecule	"high" temperature relaxation				"low" temperature relaxation			
		C_{HT} $\cdot 10^9\ s^{-2}$	E_A kJ/mol	α	τ_{CO} $\cdot 10^{-12}$ s	C_{LT} $\cdot 10^9\ s^{-2}$	E_A kJ/mol	α	τ_{CO} $\cdot 10^{-12}$ s
2	CH_3NH_2	2.6	36.6	0.4	0.02	1.1	12.5	0.1	0.09
6	$(CH_3)_2NH$	1.1	30.8	0.3	0.02	1.3	5.9	0.2	3.8
7	$(CH_3)_3N$	1.1	23.0	0.2	1.5	4.9	11.3	0.5	0.07
8	$(CH_3)_4N^+$	1.9	22.5	0.6	0.03	4.7	13.3	0.5	0.26
9	NH_3	2.6	23.3	0.7	0.06	4.2	16.6	0.5	0.10

solvated by neutral NH_3 molecules were estimated. Such a model would also explain the unusual orientation of NH_3, CH_3NH_2, and $(CH_3)_2NH$, which is unfavourable for charge transfer between the nitrogen lone pair orbital and the NbS_2 layers, but determined by ion-dipole interaction between guest species. Finally, the value of the quadrupole coupling constant of the amino deuterons suggests that intermolecular hydrogen bonds exist.

4.3. Molecular Motions within the Layers

As described above, the spectra of the amines at room temperature are determined by intramolecular fields which are greatly influenced by translation, molecular reorientation, CH_3 rotation and proton exchange. Upon cooling, these motions slow down and become finally frozen. At a temperature of 77 K the second moments of intercalated CH_3NH_2 and $(CH_3)_4N^+$ have more or less reached their rigid lattice values, which is not the case for $(CH_3)_2NH$, $(CH_3)_3N$ and NH_3. The CH_3 rotation of the last-named amines freezes at a temperature below 77 K, which can also be concluded from the spin-lattice relaxation data, if one examines the numerical values of Table 2.

From the NMR point of view it is interesting to ask why the resolved three-spin system signal of rotating methyl protons was not yet observed in other materials. The situation is probably similar to that of water in metal disulfide interlayer compounds, where averaging of the intermolecular dipole-dipole interaction resulted in the occurrence of a nearly perfect "Pake doublet" [2]. In case of the amines, and particularly if there are not too many methyl groups in the molecule, we have more or less isolated three-spin systems, where, above a certain temperature, intermolecular local fields are averaged and only intramolecular interactions persist. The fact that the we do not find three-spin and two-spin signals for the NH_3 and NH_2 protons, respectively, clearly indicates rapid proton exchange with exchange rates above 10 kHz [4]. Recently we have indeed observed well-resolved three-spin signals for NH_3, but for ammonia solvated by alkali cations in order to suppress protolysis: in $Li(NH_3)_2C_x$, $Li_{0.8}(NH_3)_{0.8}MoS_2$ [24] and $Cs_{0.3}(NH_3)_xNbS_2$ [25].

Dipolar fluctuations determine the spin-lattice relaxation rates. The values of the low temperature relaxation strength C_{LT} (Table 2) appear too small as compared with the theoretical value of $7.8 \cdot 10^9\ s^{-2}$ which should at least be reached for $(CH_3)_3N$ and $(CH_3)_4N^+$ having methyl protons only. This is probably connected with the occurrence of distribution parameters α being much smaller than 1. Since relaxation by hindered rotation of methyl groups has always shown BPP behaviour, if quantum effects were absent, the irregularity of all our low temperature relaxation peaks looks surprising at first glance. The reason may be that the local environments of the methyl groups, which are particularly determined by the host lattice, are different within the layers, in contrast to the methyl sites of molecular crystals. The values of the activation energy for CH_3 rotation have the usual order of magnitude; it is, however, not clear why the rotation is less hindered in dimethylamine.

The exceptional behaviour of the low temperature relaxation of NH_3, cf. Table 2, needs special attention. Although the assignment of the peak is not quite certain, the somewhat higher activation energy compares well with activation energies usually found for relaxation by NH_3 and CH_3

rotation. The activation energy for the motion of NH_3 molecules within the NbS_2 layers ("high" temperature peaks) does not agree with what was found for the translational diffusion in TaS_2 by quasi-elastic neutron scattering [26]. Our smaller value of 23 kJ/mol as compared to 40 kJ/mol for the translational motion may indicate that the relaxation peak is greatly determined by reorientation. Further studies of ammonia intercalated in various host lattices are in progress in order to explain the different behaviour of $NH_3[NbS_2]$ and $NH_3[TaS_2]$.

The asymmetry of the high temperature relaxation of the methylamines is less surprising since distinction between molecular reorientation and translation is not unequivocal. The results can be compared with those of bilayer hydrates in layered chalcogenides [3, 4], where translational diffusion is accompanied by changes of the orientation of the water molecules. Only samples not loaded completely with ammonia displayed dominant two-dimensional diffusion like those of monolayer hydrates. The values of C_{HT} mirror the contributions of all protons in the molecule with a motionally reduced local field of the methyl protons. Therefore $C_{HT} < C_{LT}$ holds when the same protons are responsible for both relaxation mechanisms as in trimethylamine, tetramethylammonium and ammonia itself. The succession of activation energies shows that the molecules with the lone pair orbital parallel to the layers are located in deeper potential troughs.

[1] R. Schöllhorn, Angew. Chem. **92,** 1015 (1980); Angew. Chem. Int. Ed. Eng. **19,** 983 (1980).
[2] U. Röder, W. Müller-Warmuth, and R. Schöllhorn, J. Chem. Phys. **70,** 2864 (1979).
[3] U. Röder, W. Müller-Warmuth, and R. Schöllhorn, J. Chem. Phys. **75,** 412 (1981).
[4] U. Röder, W. Müller-Warmuth, H. W. Spiess, and R. Schöllhorn, J. Chem. Phys. **77,** 4627 (1982).
[5] R. Schöllhorn and H. D. Zagefka, Angew. Chem. **89,** 193 (1977); Angew. Chem. Int. Ed. Eng. **16,** 199 (1977).
[6] B. G. Silbernagel and F. R. Gamble, Phys. Rev. Lett. **32,** 1436 (1974).
[7] F. R. Gamble and B. G. Silbernagel, J. Chem. Phys. **63,** 2544 (1975).
[8] B. G. Silbernagel, M. B. Dines, F. R. Gamble, L. A. Gebhard, and M. S. Whittingham, J. Chem. Phys. **65,** 1906 (1976).
[9] B. G. Silbernagel and F. R. Gamble, J. Chem. Phys. **65,** 1914 (1976).
[10] H. T. Weaver, J. E. Schirber, and B. G. Silbernagel, Sol. State Comm. **28,** 21 (1978).
[11] R. L. Kleinberg and B. G. Silbernagel, Sol. State Comm. **33,** 867 (1980).
[12] A. Abragam, The Principles of Nuclear Magnetism, Oxford Univ. Press (Clarendon), London 1961.
[13] E. R. Andrew and R. Behrson, J. Chem. Phys. **18,** 159 (1950).
[14] G. E. Pake, J. Chem. Phys. **16,** 327 (1948).
[15] R. G. Barnes, Advances in Nuclear Quadrupole Resonance **1,** 335 (1974), Heyden and Sons, London.
[16] D. T. Edmonds, Physics Report **29 C,** 4 (1977).
[17] N. Bloembergen, E. M. Purcell, and R. V. Pound, Phys. Rev. **73,** 679 (1948).
[18] A. Avogadro and M. Villa, J. Chem. Phys. **66,** 2359 (1977).
[19] E. Göbel, W. Müller-Warmuth, H. Olyschläger, and H. Dutz, J. Magn. Reson. **36,** 371 (1979).
[20] W. Otte and W. Müller-Warmuth, J. Chem. Phys. **72,** 1749 (1980).
[21] J. Diaz Santanilla, G. Fritsch, and W. Müller-Warmuth, Z. Lebensm. Unters. Forsch. **172,** 173 (1981).
[22] T. K. Halstead, K. Metcalfe, and T. C. Jones, J. Magn. Reson. **47,** 292 (1982).
[23] J. L. Bjorkstam and M. Villa, Magn. Reson. Rev. **6,** 1 (1980).
[24] G. Aselmann, Diplomarbeit, Münster 1982, unpublished.
[25] E. Wein, Münster 1982, unpublished work.
[26] C. Riekel, A. Heidemann, B. E. F. Fender, and G. C. Stirling, J. Chem. Phys. **71,** 530 (1979).